Available online at www.sciencedirect.com
SCIENCE DIRECT®
Journal of Hydrology 308 (2005) 196–213
Journal of Hydrology
www.elsevier.com/locate/jhydrol

Tree-ring footprint of joint hydrologic drought in Sacramento and Upper Colorado river basins, western USA

David M. Meko[a,*], Connie A. Woodhouse[b,1]

[a]*Laboratory of Tree-Ring Research, University of Arizona, Tucson, AZ 85721, USA*
[b]*Paleoclimatology Branch, NOAA National Climatic Data Center, 325 Broadway, E/CC23, Boulder, CO 80305, USA*

Received 9 October 2003; revised 30 October 2004; accepted 5 November 2004

Abstract

Growing and changing demands on water supply, along with natural climate variability and possible anthropogenically induced climate change, make water resource management and planning increasingly challenging, particularly in arid regions. Instrumental climate and gaged streamflow records provide just a snapshop of recent natural hydrologic variability. In this paper, we use tree-ring-based annual streamflow reconstructions for the Sacramento River in California and the Blue River in western Colorado to analyze the temporal and spatial variability of widespread drought simultaneously affecting both basins over the past five centuries. Stability of joint-drought episodes and the covariation of reconstructed flows in the two basins are analyzed with sliding correlations, spectral analysis and a hypergeometric test. Year-to-year spatial patterns of moisture anomalies in a singular joint-drought episode in the late-1500s are mapped with a network of tree-ring data. Climatological aspects of joint droughts of the 20th century are investigated with 500-mb geopotential height data and climatic indices.

Although flow in the two rivers is only very weakly correlated over the full 538-yr reconstruction period, more years of joint drought occur than would be expected by chance alone. Covariation in reconstructed flows is stronger in the late 1500s and mid-1700s than at any time since 1800. The late 1500s period of drought is not characterized as a decades-long unbroken drought, but as a series of drought impulses broken by wet years, with widespread moisture deficits in joint dry years. Periods of high inter-basin correlation in reconstructed flow are characterized by coherency at frequencies within the ENSO band. However, joint droughts in instrumental gage records do not display any consistent relationship with ENSO or the Pacific Decadal Oscillation (PDO), and so it is difficult to infer either as a causal mechanism for joint droughts in the past.

Keywords: Paleoclimatology; Drought; Runoff; Tree rings; Western US; ENSO

1. Introduction

Demands for fresh water supplies have escalated in many areas of the world as a result of burgeoning populations and expanding economies. Semi-arid and arid regions are particularly vulnerable to

* Corresponding author. Tel.: +1 520 621 3457; fax: +1 520 621 8229.
E-mail addresses: dmeko@ltrr.arizona.edu (D.M. Meko), connie.woodhouse@noaa.gov (C.A. Woodhouse).
[1] Tel.: +1 303 497 6297; fax: +1 303 497 6513.

0022-1694/$ - see front matter © 2004 Elsevier B.V. All rights reserved.
doi:10.1016/j.jhydrol.2004.11.003

water-related stresses and shortfalls. As water management agencies in these areas work to meet demands, they must also deal with the effects of natural climate variability on water supplies as well as future uncertainties due to impacts of global warming on regional climate. General circulation model projections based on increased greenhouse gases indicate changes in frequency, intensity and duration of extreme events, leading to increased risk of drought in many regions. Increased summer dryness in mid-latitude continental interiors is considered likely, with increased probability of drought (IPCC, 2001).

The issues related to water management in the semi-arid western United States represent an example of the challenges that are being faced by water managers worldwide. Competing demands of urban and rural/agricultural water users, expanding water needs that now include recreation and maintenance of in-stream flows, and a limited water supply, coupled with a recent, severe and widespread 2002 drought that caught many water managers by surprise (Loomis et al., 2003; Rider, 2003) have caused water planning agencies to re-evaluate water systems and their ability to meet demands in coming decades.

The impacts of drought can be mitigated through knowledge and planning that considers underlying natural climate variability. Management can benefit from increased understanding of the spatial and temporal aspects of climate that affect regional water supplies, including the differential impacts of climate across multiple basins within a region. Knowledge about the statistical likelihood of extreme events, and their evolution in time and space, is critical as well. As important is knowledge of the possible association of such events with recognizable features of variability of the earth-atmosphere system, such as the well-known El Niño/Southern Oscillation (ENSO) and Pacific Decadal Oscillation (PDO) phenomena.

Instrumental climate and gaged streamflow records provide some basis for understanding natural hydrologic variability. However, such records are typically limited in length to 100 yr or less, and so afford only a snapshot of possible variability. The paleoclimatic record for western North America suggests strongly that earlier droughts were more severe and widespread than any in the period covered by gaged records. A drought covering large parts of northern Mexico and the western United States, for example, reportedly lasted more than a decade in the late 1500s (Stahle et al., 2000).

In this paper, we examine paleoclimatic records for information on temporal and spatial variability of widespread drought simultaneously affecting the Sacramento and Colorado river basins, two important sources of surface water in the western United States. We focus on the episodes of joint drought, defined here as low annual flows in both basins. We analyze the long-term stability of joint-drought episodes and the covariation of reconstructed flows in the two basins, and apply the existing large-scale network of tree-ring chronologies in the western United States and northern Mexico to infer year-to-year evolution of spatial patterns of moisture anomaly in the late-1500s drought. We also examine possible statistical links with climatological indices and circulation patterns.

2. Study area

The two river basins that are the focus of this study are the Sacramento River Basin, California, and the Blue River Basin, Colorado (Fig. 1). These basins were selected for their strategic importance to water supply in the western United States and the availability of long-term (500+years) tree-ring reconstructions of annual flow. The Sacramento River is the largest in-state source of surface water for California, making up 30% of the flow of all rivers in the state (Crippen, 1986). The Blue River is an important source of water supplies for the two main water providers in the Front Range metropolitan region—the Denver Water Board and the Northern Colorado Water Conservancy District. Both water utilities use the Blue River gage record, with other gages, to characterize historical and current water supply.

Although separated geographically by 1200 km, the two basins are components of a vast water-supply network tapped by southern California. Besides in-state resources, California relies on the Colorado River, of which the Blue River is a tributary, for approximately 12% of its total annual agricultural and urban water supply (Cayan et al., 2003). Cool-season precipitation and snowmelt are important components of the runoff in both basins. Although the climatic regimes and controls in the two basins are different,

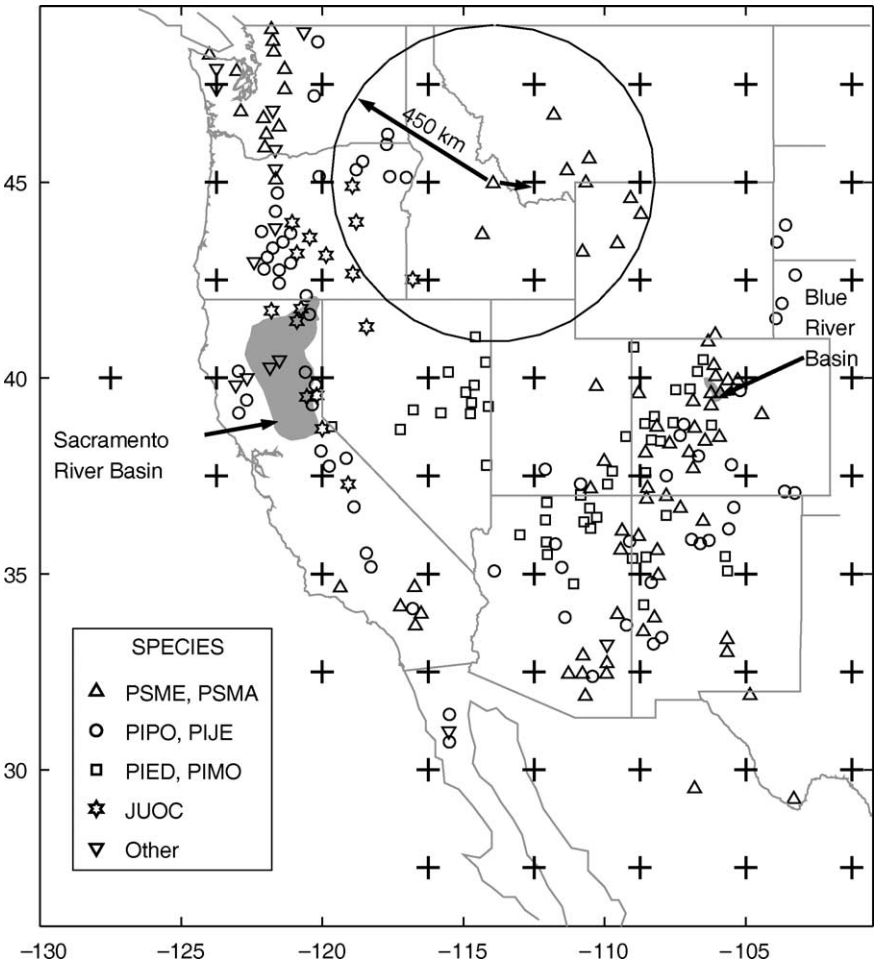

Fig. 1. Map showing locations of tree-ring sites, river basins, and precipitation gridpoints. Tree-ring sites symbol-coded by species: PSME, *Pseudotsuga menziesii*; PSMA, *Pseudotsuga macrocarpa*; PIPO, *Pinus ponderosa*; PIJE, *Pinus jeffreyi*; PIED, *Pinus edulis*; PIMO, *Pinus monophylla*; JUOC, *Juniperus occidentalis*. River basins shaded. Precipitation gridpoints marked with '+'. Circle in central Idaho illustrates search radius for screening tree-ring chronologies with gridded precipitation (see text).

recent work indicates that dry years often have widespread impacts across both basins, and tend to persist over time (Cayan et al., 2003).

3. Data

3.1. Hydrologic and climatic data

Streamflow data used in the study are water-year (October–September) totals of 'natural flow', which has been adjusted for removal of effects of reservoir storage, irrigation withdrawals, and other distortions related to development of the basin. Natural flows for the Sacramento River, 1906–2002, were obtained from the California Department of Water Resources (CADWR, 2003). The series, referred to from here on as SAC, is the sum of Sacramento River at Bend Bridge, Feather River inflow to Lake Oroville, Yuba River at Smartville, and American River inflow to Folsom Lake. Natural flows for the Blue River above Dillon Reservoir, referred to from here on as BLU, for the period 1916–2002 were obtained from the Denver Water Board and are available online from the NOAA Paleoclimatology Branch (NOAA, 2003a).

Table 1
Statistics of observed annual flows

Basin	Area (km^2)	Period	Basic statistics[a]			Quantiles[b]		
			Mean	*S*	cv	0.1	0.2	0.5
Sacramento R.	41,000	1906–2002	22.2468	9.5881	0.43	49.3	60.9	92.0
Blue R.	331	1916–2002	0.2813	0.0737	0.26	68.0	82.2	96.2

[a] Mean (km^3/yr), standard deviation (km^3/yr), and coefficient of variation; computed from annual (water-year) flows.
[b] Quantiles of annual flow as percentage of mean.

BLU is a much smaller watershed than SAC: the ratio of basin areas is less than 0.01, and the ratio of mean annual flows is only slightly greater than 0.01 (Table 1). Nevertheless both series can be regarded as indicators of large-scale hydrologic conditions. BLU depends heavily on snowmelt, whose anomalies, especially deficits, over the west slope of the Rockies might be expected to be large in spatial extent. BLU correlates quite strongly ($r=0.702$, $N=86$, p-value $\leq 1\times10^{-8}$) with the flow of the Colorado River at Lees Ferry for the period 1916–2001.

Precipitation data were extracted from a global land-based gridded (2.5° latitude by 3.75° longitude) precipitation dataset (Hulme et al., 1998). Monthly values, 1901–1964, for 58 gridpoints in the western United States and northern Mexico (Fig. 1) were obtained from Hulme (2000) and converted to water-year totals for use in the study.

Two indices of winter Pacific sea-surface temperature (SST) were used in this study. The Niño 3.4 index, an area-average of SST over 170°W–120°W, 5°S–5°N for the period 1871–2000, was obtained from Stepaniak (2002), and extended through water-year 2002 with data from Climate Prediction Center (NOAA, 2003b). This index measures anomalous SST in the eastern equatorial Pacific, and is strongly related to ENSO variations (Trenberth and Stepaniak, 2001). The Pacific Decadal Oscillation (PDO) index, 1900–2002, was obtained from Mantua (2003). The PDO is an index of the primary mode of spatial variability of SST in the Pacific Ocean north of 20°N and is thought to be associated with 'regime changes' in climate of western North America that occurred most notably in the early 1940s and late 1970s (Mantua et al., 1997). The warm phase of the PDO is associated with warm SST in the North Pacific off the coast of North America. Niño 3.4 and PDO indices were downloaded as monthly data and averaged over winter months December–March.

Maps of 500-mb geopotential height anomalies (NCEP/NCAR Reanalysis) for Oct–May were downloaded from the NOAA CIRES Climate Diagnostics Center (NOAA, 2003c).

3.2. Paleoclimatic data

Tree-ring reconstructions of water-year-total natural flow for SAC and BLU were analyzed for this study. The reconstruction for SAC, A.D. 901–1977, was generated by Meko (2001) for the California Department of Water Resources from existing tree-ring chronologies supplemented by new field collections in the late 1990s, and updates an earlier published reconstruction (Meko et al., 2001). The reconstruction for BLU, A.D. 1440–1999, was generated for the Denver Water Board by Woodhouse et al. (2003). Regression statistics indicate the reconstructions for both basins are of relatively high quality compared with other published tree-ring reconstructions: 67% of the variance of the annual flows (1906–1977) on the Sacramento River, and 62% of the variance (1916–1999) on the Blue River are accounted for by the reconstruction models. Both reconstructions are available online from the World Data Center for Paleoclimatology (NOAA, 2003a).

This study also makes use of a continental-scale network of tree-ring data to infer year-by-year spatial patterns of moisture anomalies during the severe drought of the late 1500s. Annual ring widths for all chronologies of likely drought-sensitive species with time coverage A.D. 1575–1964 in the region 29°–49°N, 103°–124°W were downloaded from the International Tree-Ring Data Bank (NOAA, 2003d). Raw measurement series were standardized by

detrending with a negative exponential, straight line, or a cubic smoothing spline with 50% response at a wavelength 2/3 the sample length to remove the growth trend while preserving as much of the low frequency information as possible (Cook et al., 1990). Each 'site chronology' represents tree-ring anomalies averaged over many trees. The network comprises 217 chronologies, representing 11 different species (Fig. 1). The most common species in the network are *Pseudotsuga menziesii* (70 chronologies), *Pinus ponderosa* (56 chronologies), and *Pinus edulis* (32 chronologies). The autoregessive-residual form of the chronologies was used to avoid large site-to-site biologically driven differences in chronology autocorrelation.

4. Methods

4.1. Tree-ring screening

Tree-ring chronologies with a moisture signal were selected by a correlation analysis with gridded water-year-total precipitation. Each chronology in the 217-site network of candidate sites was correlated with precipitation, 1901–1964, at gridpoints within a 450 km radius (Fig. 1). The number of gridpoints for the correlation analysis varies by tree-ring site. For example, the annotated search radius around the chronology in north-central Idaho in Fig. 1 encompasses seven gridpoints. A chronology was accepted as moisture-sensitive if median correlation with all gridpoints in the search radius was positive and either of the following null hypotheses could be rejected: (1) correlation with nearest gridpoint is zero, or (2) correlation with each of the gridpoints in the search radius is zero. An α-level of 0.05 was used for the first test, and a Bonferroni-adjusted α-level of $0.05/m$ was used for the second test, where m is the number of gridpoints in the search radius. This dual criterion for rejection allows for the possibility that the nearest gridpoint is less representative than some other gridpoint of precipitation variations at the tree-ring site. The use of a modified α-level for the second test reduces the chance of spuriously high correlation due to multiple comparisons.

4.2. Smoothing and correlation

Time series were smoothed to emphasize variations at decadal-and-longer time scales with a 19-weight Gaussian filter (weights: 0.0067, 0.0119, 0.0199, 0.0310, 0.0450, 0.0612, 0.0776, 0.0920, 0.1019, 0.1054, 0.1019, 0.0920, 0.0776, 0.0612, 0.0450, 0.0310, 0.0199, 0.0119, 0.0067). The frequency response of this filter is 0.5 at a wavelength of 20 yr and drops below 0.05 at wavelengths shorter than 10 yr. The degree of smoothing is comparable to that of an evenly weighted 11-yr moving average, which has a frequency response of 0.5 at a wavelength of about 18 yr.

The strength of linear relationship between pairs of time series was measured by the product–moment correlation coefficient, and significance of correlation was evaluated by a '*t*' test (Snedecor and Cochran, 1989, p. 187). Correlations were also computed in a sliding time window to evaluate possible time-dependence of correlation. To adjust for possible effects of autocorrelation on degrees of freedom, the effective sample size for correlation as defined by Dawdy and Matalas (1964) was used in computing thresholds for significance. The significance of the difference of two sample correlations for non-overlapping windowed segments was tested using a normal distribution after Fisher transformation of the correlation coefficients (Snedecor and Cochran, 1989, p. 189).

4.3. Definition and statistical significance of occurrence of joint drought

A joint-drought year was defined as a year when both SAC and BLU were below some defined threshold–either a particular quantile of the flow series or a specified percentage of mean flow. This same definition was applied to Gaussian-smoothed annual flow series to identify extended joint-drought periods.

The probability of obtaining the observed number of joint-drought years by chance if two series are unrelated was estimated using a hypergeometric distribution (Conover, 1980; Dracup and Kahya, 1994). The test based on this distribution gives the probability of k or more successes in n trials from a finite population of size N containing m successes. In

our application, N is the number of years in the period of analysis, n is the number of years the first series is below its q quantile (e.g. 0.2 quantile), and $m=n$ is the number of years the second series is below its q quantile. A success is defined as both series below their q quantile in the same year.

4.4. Spectrum and cross-spectrum

Spectra and cross-spectra of time series were estimated by the smoothed-periodogram method (Bloomfield, 2000). Analyses were conducted both for the full-length streamflow reconstructions (538 yr), and for the reconstructions in a sliding time window (101 yr). Specific processing choices for our analysis include: (1) series were initially detrended and converted to zero-mean by fitting and removing a least-squares-fit straight line, (2) the ends of the time series (5% of the observations on each end) were tapered with a cosine-bell taper to reduce possible effects of 'leakage' on the estimated spectrum (Bloomfield, 2000, p. 66), (3) series were padded to a length equal to the next power of two greater than the original series length by appending zeros to facilitate use of the fast Fourier transform, (4) the spectrum was estimated by smoothing the periodogram with a sequence of a Daniell filters chosen to give a desired bandwidth for the spectral estimates (likewise this smoothing was applied to the cross-periodogram to estimated the cross-spectrum).

Different filters were used to smooth the periodogram depending on the series length. For the full-length analysis (original length 538 yr, padded length 1024 yr), the filter was a convolution of three individual 41-weight Daniell filters (Bloomfield, 2000, p. 152). For the windowed analyses (original length 101 yr, padded length 128 yr), the filter was a convolution of three five-weight Daniell filters. Following Chatfield (1975, p. 154) we defined the bandwidth of the spectral estimator as the width of the rectangular filter that has approximately the same variance as the filter used to smooth the periodogram. By this definition, the spectral bandwidth is 0.07 yr^{-1} for the 538-yr analysis and 0.06 yr^{-1} for the 101-yr analysis.

Confidence intervals for spectra were computed by assuming the spectral estimates approximately follow a χ^2 distribution whose degrees of freedom are a function of the sum of squares of weights in the filter used to smooth the periodogram—with adjustment for any padding or tapering used in the analysis (Bloomfield, 2000, p. 184). The confidence interval for the squared-coherency, C^2, was computed on the assumption of a normal distribution for C^2 after arctanh transformation to stabilize variance. The confidence interval for the phase was computed on the assumption that the phase is approximately normally distributed when C^2 is significantly greater than zero. Equations for the confidence intervals for these cross-spectrum functions can be found in Bloomfield (2000, p. 218–221).

The confidence intervals for phase and squared coherency are applicable only when the squared coherency is significantly greater than zero. Accordingly, the confidence intervals are plotted only for frequencies at which squared coherency exceeds

$$C^2_{.05} = 1 - 20^{-g^2/(1-g^2)}$$

where g^2 is the adjusted (for tapering and padding) sum-of-squares of weights of the Daniell filter used to smooth periodograms and cross-periodograms (Bloomfield, 2000, p. 221).

5. Results and discussion

5.1. Identification of joint-drought episodes

5.1.1. Observed record

The coefficient of variation and the flow quantiles expressed as percentage of mean flow indicate that, after scaling to compensate for difference in means, BLU is much less variable than SAC (Table 1). This difference in variability is also evident in the time series plots of the observed flows (Fig. 2). Flows less than half the long-term mean occur 11 times in SAC but just two times in BLU in the common period 1916–2002. This result is consistent with the findings of Cayan et al. (2003) that interannual variability of annual flow is generally greater in the Sierra Nevada watersheds than in the Upper Colorado watersheds. Cayan et al. (2003) also note that the difference in variability appears to be independent of basin size.

Frequency of joint-drought episodes naturally depends on the flow threshold used to define drought.

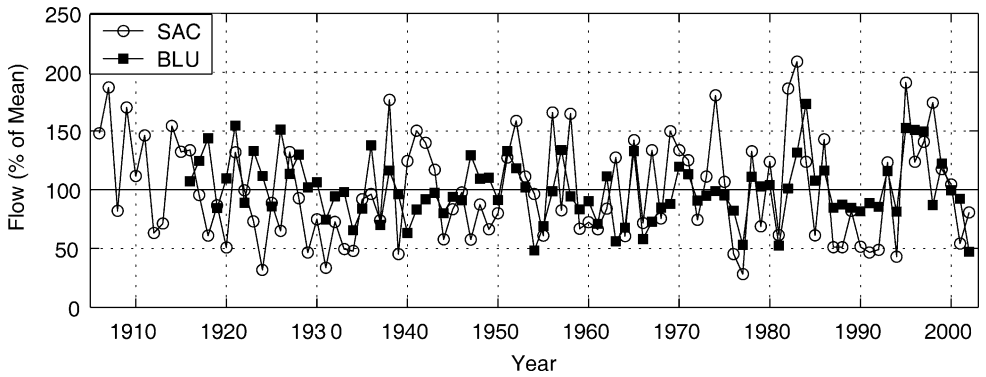

Fig. 2. Time series plots of observed annual flows of Sacramento River and Blue River. Series defined in text, and plotted as percentage of 1906–2002 (Sacramento) and 1916–2002 (Blue) means.

By the 0.1 quantile (Table 1), only 1934 and 1977 are joint-drought years. By the 0.2 quantile, three additional years are classified as joint drought: 1931, 1990, and 1994. By an even less stringent threshold of 0.25 quantile, four more years enter: 1944, 1964, 1955 and 1976.

Given the importance of storage on the river systems in the Colorado and Sacramento basins, it is also meaningful to consider as joint droughts periods with below normal flow averaged over multi-year periods. The 6-yr running means of the two observed flow series are simultaneously below their 0.2 quantiles three times: 1930–1935, 1976–1981, and 1987–1992. The most recent of these periods, an ecologically devastating drought in California (Gleick and Nash, 1991), was characterized by six consecutive years below the mean in both series (Fig. 2). With increasing length of averaging period, the minima in SAC and BLU become less synchronous. For example, by a tally of 20-yr running means there are no joint droughts in the observed record.

5.1.2. Reconstructed record—smoothed

SAC and BLU reconstructions smoothed with the 20-yr Gaussian filter emphasize variations at decadal and longer time scales (Fig. 3). Low-frequency variations in SAC and BLU are generally out of phase since the mid-1800s, but not so over the entire reconstruction. For example, the series appear to be in-phase from the late 1600s to late 1700s.

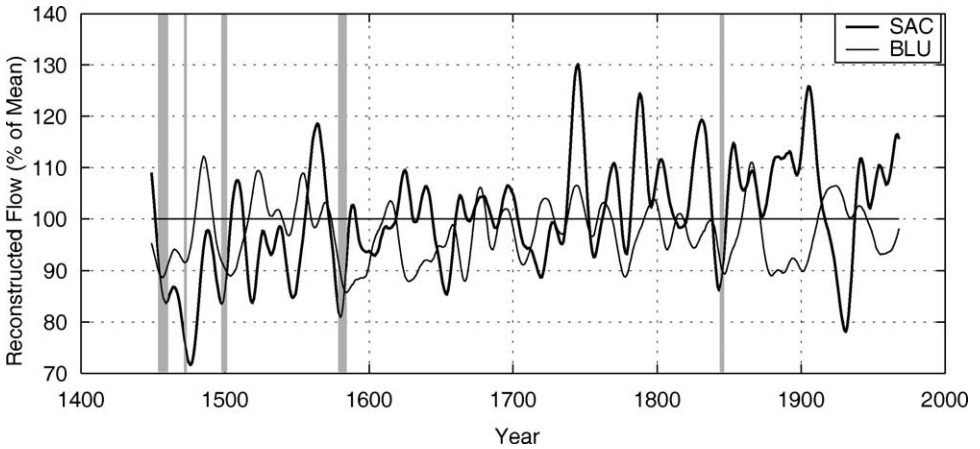

Fig. 3. Smoothed time series of annual flows of Sacramento River and Blue River reconstructed from tree rings, 1440–1977. Series converted to percentage of 1916–1977 mean and then smoothed with 20-yr Gaussian filter (frequency response 0.5 at wavelength 20 yr). Periods with both smoothed series below 0.2 quantile shaded.

Fluctuations in-phase and out-of-phase cancel in the long run, such that the correlation of the smoothed SAC and BLU series over the full reconstruction period is approximately zero ($r=0.02$).

Joint droughts as defined by smoothed flows below the 0.2 quantile in both series are rare events. Five distinct drought periods are identified by shading in Fig. 3: 1454–1460, 1472–1473, 1498–1501, 1579–1584, and 1844–1846. The North American 'mega-drought' of the late 1500s (Stahle et al., 2000) is characterized by all-time low flow on BLU, and flow on SAC that is lower than at any time except the late 1400s and the 1930s. The most recent occurrence of joint drought in the smoothed reconstruction is the 1840s.

5.1.3. Reconstructed record—unsmoothed

The reconstructions are valuable for their information on low-frequency fluctuations in streamflow because those fluctuations are not amenable to analysis with the relatively short gaged record. However, useful information can also be extracted on frequency of single-year and multi-year events, and for this we must analyze the unsmoothed, or original, reconstructions. A listing of years with SAC and BLU simultaneously below the 0.2 quantile identifies several interesting clusters of drought years (Table 2). Examples are the triplets of consecutive joint-dry years in 1652–1654 and 1735–1737. These clusters did not emerge in the preceding analysis (smoothed reconstruction) because the Gaussian filter used deemphasizes droughts much shorter than the filter length. In comparison, the 20th century part of the reconstructions contains no instances of consecutive years below the 0.2 quantile.

Table 2
Joint-drought[a] years in SAC and BLU reconstructions

1440–1600	1601–1800	1801–1977
1475*	1607*	1846
1480	1622*	1871
1499*	1646	1898*
1500*	1652	1959
1515	1653*	1961*
1532	1654*	1977
1580*	1686	
1581	1729*	
1584	1735	
1585	1736	
1590*	1737	
1600*	1756	
	1765	
	1770	
	1777*	
	1795	

[a] All years with BLU and SAC below 0.2 quantile are listed; those below 0.1 quantile marked with asterisk.

The ranking, and indeed the identification, of past joint droughts is clearly sensitive to the method of statistical summary. Some periods are jointly dry, however, whether evaluated with the smoothed or unsmoothed reconstructions. The most notable of these is the late 1500s. The period 1579–1584 is one of five joint droughts in the smoothed series (Fig. 3), and six of the 34 individual joint-dry years in the full 1440–1977 reconstructions occur between 1580 and 1600 (Table 2).

The hypergeometric test addresses the question whether the frequency of joint-drought years in SAC and BLU is statistically larger than expected by chance for two independent time series. The results of the hypergeometric test for significance of joint occurrence of individual drought years on SAC and BLU are listed in Table 3. For the observed data, 1916–2002, results indicate that joint occurrence of flows below the median is greater than expected by chance. Twenty-nine of 44 dry years on SAC were also dry years on BLU. The probability of 29 or more matches for unrelated time series by chance alone is 0.0035. Contingency-table analysis of annual-flow series from Sierra Nevada and Colorado Basin watersheds similarly shows a tendency for coincidence of low-flow years (lowest tercile) on a more regional scale (Cayan et al., 2003).

On the other hand, the frequency of joint-drought years in the observed data does not reach significance for the more stringent 0.1 and 0.2 drought quantiles. Moreover, the sensitivity of the results to the choice of sample period is evident in the differing results for the 0.5-quantile test for the 1916–1977 and 1916–2002 base periods. These results are likely due to the small sample sizes available for the observed series. For example, the 0.1 quantile for the 1916–2002 data classifies only 9 yr as drought years in the individual series, but the 538-yr reconstructed flow series provides stronger support for co-occurrence of flows below the 0.1 and 0.2 thresholds. At the 0.1 quantile, 14 of 54 drought years on SAC were also drought

Table 3
Probabilities of observed joint-drought frequency estimated from hypergeometric distribution

Data type	Period	N[a]	0.1 Quantile			0.2 Quantile			0.5 Quantile		
			n[b]	k[c]	p[d]	n[b]	k[c]	p[d]	n[b]	k[c]	p[d]
Observed	1916–2002	87	9	2	0.2330	17	5	0.2065	44	29	0.0035
	1916–1977	62	6	1	0.4718	12	4	0.1673	31	18	0.1548
Reconstructed	1916–1977	62	6	1	0.4718	12	5	0.0443	31	20	0.0207
	1440–1977	538	54	14	0.0003	108	34	0.0011	269	153	0.0009

[a] Number of years in sample.
[b] Number of years each series below indicated quantile.
[c] Number of matches, or number of years both series below indicated quantile.
[d] Probability of k-or-more matches by chance alone when no relationship.

years on BLU. The probability of 14 or more matches by chance alone is 0.0003. Note however that the fraction of matches is only slightly higher than in the observed data (14/54 vs 2/9), so that the added significance comes from the greater sample size rather than a marked increased frequency for joint droughts in the past. This comparison demonstrates one of the benefits of the lengthened records provided by the reconstructions.

5.2. Cross-spectral analysis

The correlation between annual reconstructions of SAC and BLU, 1440–1977, is small, yet highly statistically significant by virtue of the length of the series ($r=0.18$, $N=538$, p-value$=3.1\times10^{-5}$). Because the low frequency components of SAC and BLU (plotted in Fig. 3 and discussed previously) are essentially uncorrelated, the significant correlation in the series probably originates at frequencies higher than those tracked by the 20-yr Gaussian filter.

The linear relationship between SAC and BLU as a function of frequency is summarized by the estimated squared coherency and phase functions from cross-spectral analysis (Fig. 4). The individual spectral have also been plotted to aid in the interpretation. The spectra are not particularly noteworthy, as neither differs significantly from a white-noise spectrum (Fig. 4a and b). The closest approach to statistical significance is near the 20-yr wavelength by SAC. The spectrum of the entire SAC reconstruction, A.D. 901–1977 (not shown), likewise peaks near 20 yr, though again the peak is not significant. Enhanced variance at wavelengths on the order of 20–30 yr might reflect climate variations associated with the PDO phenomenon, although the long-term properties of PDO are not as yet well established. Neither series shows particularly enhanced variance at wavelengths associated with ENSO. It should be noted, however, that the 'ENSO band' is ill-defined because ENSO is not a strictly periodic phenomenon. Spectral analysis of station pressure series used in computing the Southern Oscillation Index (SOI) indicates a band broadly at 2.2–7.2 yr, with maximum signal at 2.8–3.5 yr (Julian and Chervin, 1978), while recurrence intervals of ENSO events from anecdotal evidence range from 3–4 yr for events of all intensity to 6–7 yr or more for strong events (Enfield, 1992). The variance peaks near frequencies 0.4 and 0.16 yr^{-1} in SAC could therefore plausibly reflect ENSO influence. An 'ENSO band' defined loosely as wavelengths 2–7 yr is not particularly diagnostic, as it covers about 3/4 of the entire frequency range of the spectrum. It should not be surprising to find some spectral peak within this broad band by chance alone. More noteworthy is the lack of any spectral peak in either series near the presumed heart of the ENSO band (say, 3–4 yr). The lack of a strong ENSO influence is perhaps to be expected as these watersheds are not in the main geographic zone of ENSO influence on streamflow in the western United States in the 20th century (Cayan and Peterson, 1989).

The squared coherency function, analogous to a correlation coefficient as a function of frequency, shows that that significant coherency is restricted to three bands, centered on frequencies 0.069, 0.195 and 0.438 yr^{-1} (periods 14.5, 5.2, and 2.3 yr) (Fig. 4c). Periods 5.2 and 2.3 yr could again be considered within the frequency range generally associated with ENSO, while 14.5 yr is somewhat shorter than

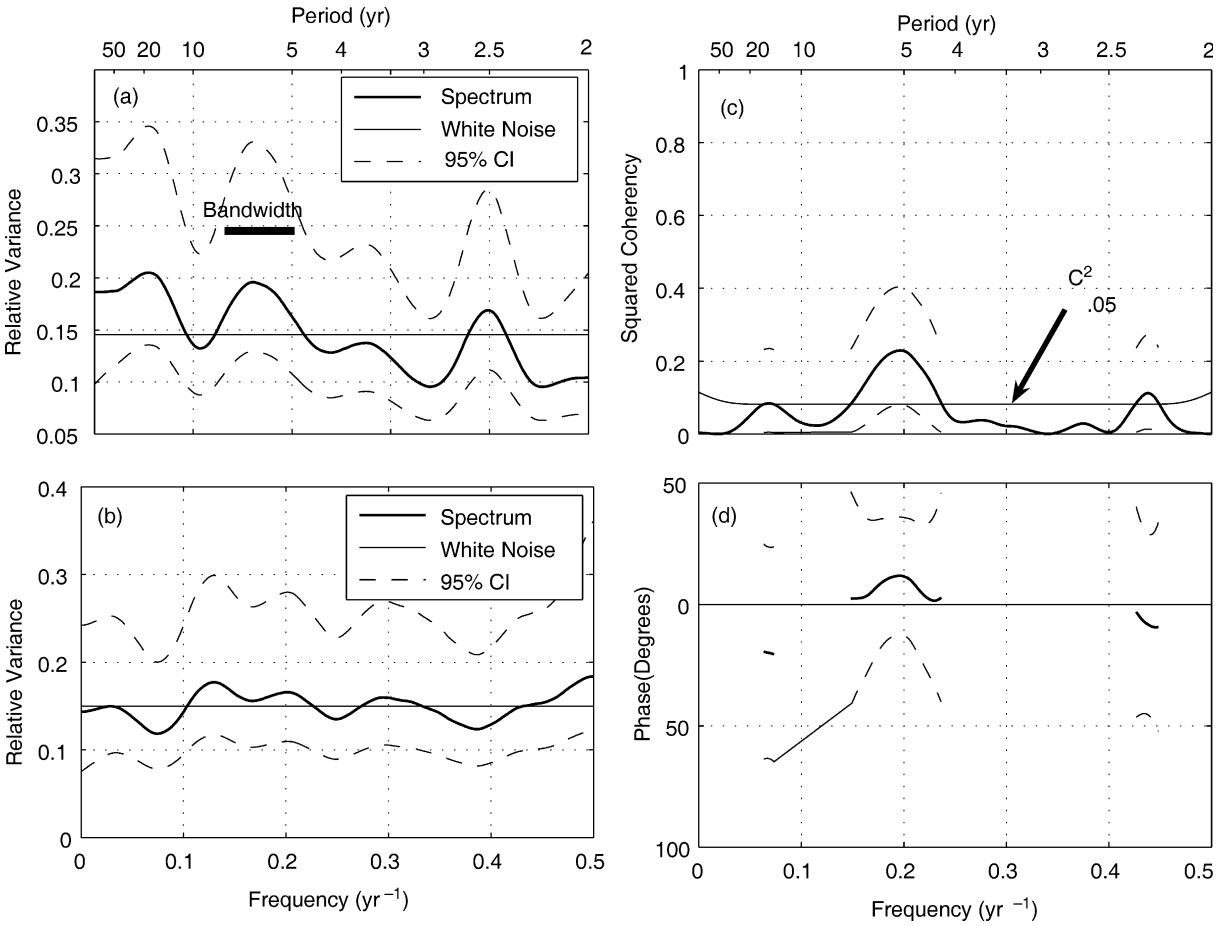

Fig. 4. Results of cross-spectral analysis of reconstructed annual flows of Sacramento River and Blue River, 1440–1977. (a) Spectrum of the SAC. (b) Spectrum of BLU. (c) Squared coherency; line annotated $C^2_{.05}$ marks threshold required to reject null hypothesis of zero coherency at 0.05 alpha-level. 95% confidence interval included for frequencies at which that hypothesis can be rejected. (d) Phase, with 95% confidence interval.

expected for PDO influence. The phase spectrum shows that within the bands of significant coherency SAC and BLU are essentially in phase (Fig. 4d). Highest coherency centers on a wavelength of about 5 yr; that the individual spectral also have high variance near 5 yr lends support to this being a real feature of the covariation.

The contrasting periods of synchrony and asynchrony in the time series of the smoothed reconstructions (Fig. 3) suggest time-dependence in the relationship between SAC and BLU. This possibility is further supported by the results of the correlation and cross-spectral analysis in a sliding 101-yr time window (Fig. 5). Adjacent windows are offset by 25 yr, and so are not completely independent of each other. The windowed correlations and an approximate critical threshold for significance (0.05 α-level, not corrected for multiple comparisons) are plotted at the top of Fig. 5. Because the first-order autocorrelation of the individual series in any windowed period is too low for the adjustment to effective sample size (Dawdy and Matalas, 1964) to have a perceptible effect on the critical threshold for significant correlation, the threshold line is approximately horizontal. Although the correlation between BLU and SAC is positive for all windowed periods,

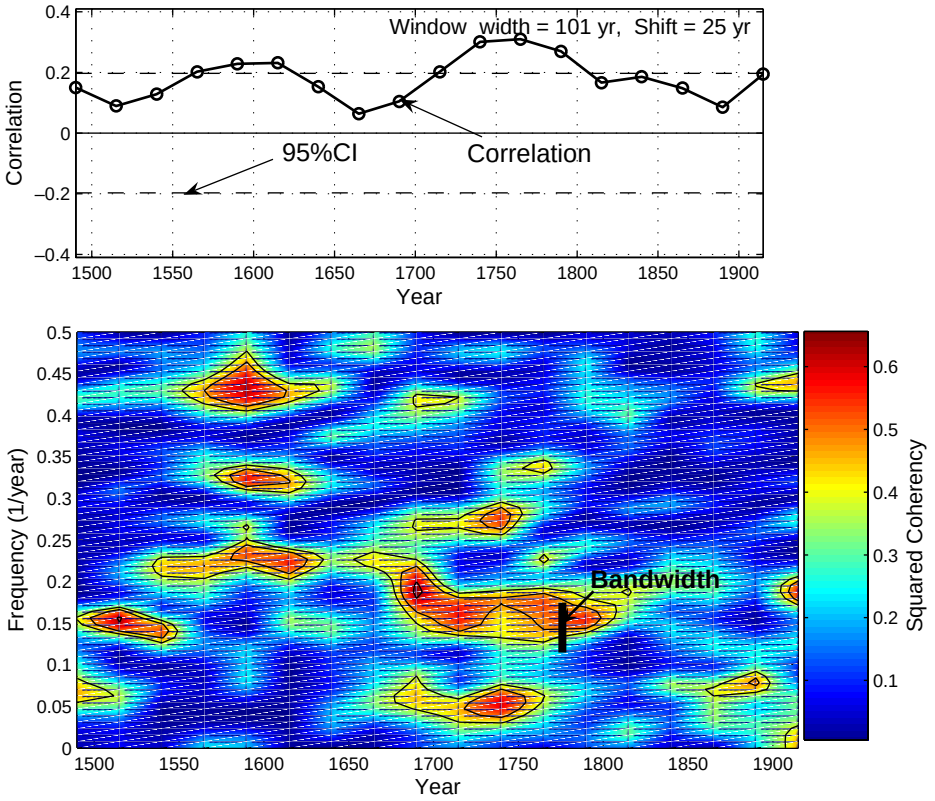

Fig. 5. Correlation and squared coherency of reconstructed SAC and BLU as a function of time. Top: product–moment correlation for 101-yr periods offset by 25 yr. Bottom: squared coherency (C^2) from cross-spectral analysis using same setting for sliding windows. Contours drawn at 90, 95 and 99% confidence levels of C^2. Plotting point on x-axis is center year of window.

statistical significance is reached only in the most recent period (barely) and in seven periods before 1800.

The observed fluctuation of windowed correlations in Fig. 5 is too small to warrant physical interpretation. Gershunov et al. (2001) caution that fairly large but physically meaningless temporal fluctuations in sliding correlations can be observed in randomly generated pairs of correlated time series. Moreover, a t-test of correlations plotted in Fig. 5 reveals that the maximum and minimum windowed correlations ($r_{1765}=0.310$, $r_{1665}=0.064$) from non-overlapping periods are not statistically different from one another at the 0.05 α-level.

Despite the lack of statistically significant fluctuation in the windowed correlations, the salient properties of the cross-spectrum vary markedly as a function of time (Fig. 5, bottom). For example, the most recent 101-yr segment has highest coherence near 5.2 yr, with secondary regions of weak coherence near 2.3 yr and at greater than 50 yr, while the segment centered on 1850 has none of these features. Two periods with relatively high coherence in multiple frequency bands are found near 1590 and 1740. Coherence appears to shift toward lower frequencies, however, from the earlier to latter period:

1590: 2.3 yr, 3.1 yr, 4.2 yr
1740: 3.6 yr, 5.7 yr, 18.5 yr

The evolutory squared coherency plot indicates that the frequencies of high coherency in the 1440–1977 cross-spectrum (Fig. 4c) originate from different subperiods of the reconstructed record. The broadest band, near 5 yr, comes mainly from the late 1600s and 1700s, when SAC and BLU also happen to reach their highest correlation. The band near 2.3 yr comes mainly from the late 1500s. The band near 14.5 yr

Table 4
Correlation of tree-ring chronologies with gridded water-year precipitation

Level[a]	Correlation	
	Nearest[b]	Median[c]
Lowest	0.21	0.06
0.25q	0.39	0.34
0.50q	0.50	0.43
0.75q	0.57	0.49
Highest	0.74	0.64

[a] Extreme or specified quantile of correlation for the 169 chronologies.
[b] Correlation with nearest gridpoint.
[c] Median correlation with all gridpoints in search radius.

comes mainly from the mid-1700s. No feature in the evolutory squared coherency is uniformly present over the full length (1440–1977) reconstruction. If we define the ENSO band loosely as wavelengths 2–5 yr, the strongest coherency in the ENSO band occurs in the late 1500s.

5.3. Epic drought of late 1500s

The late 1500s, unusual both for occurrence of joint drought and for the coherency of SAC and BLU reconstructed flows at high frequencies, was selected for a case study of year-by-year evolution of drought patterns using the 217-site tree-ring network (Fig. 1). The first step in the analysis was to cull the tree-ring chronologies to be used as proxy moisture variables.

5.3.1. Screening of tree-ring chronologies

Seventy-eight percent, or 169 of the 217 chronologies in the original tree-ring network (Fig. 1) passed the screening test for statistically significant precipitation signal. The test for correlation with precipitation at the nearest gridpoint was by itself fairly effective at screening, identifying 167 of the 169 chronologies. The remaining two chronologies entered by virtue of significant correlation with at least one chronology in the search radius. Correlation of the 169 accepted tree-ring chronologies with precipitation at the nearest gridpoint ranges from 0.21 to 0.74, and correlation for a given chronology is generally highest with the gridpoint nearest the site (Table 4). The 12 *Pinus monophylla* and *Pinus edulis* sites in Nevada are roughly midway between the SAC and BLU basins and so are critical for inferring the spatial continuity of joint droughts (Fig. 1). The correlation exceeds 0.36 for all 12 of these chronologies, and exceeds 0.44 for 11 of the 12.

5.3.2. Year-by-year evolution of drought in the late 1500s

A bar chart of the annual reconstructed streamflow as percentage of mean shows that the late 1500s is not

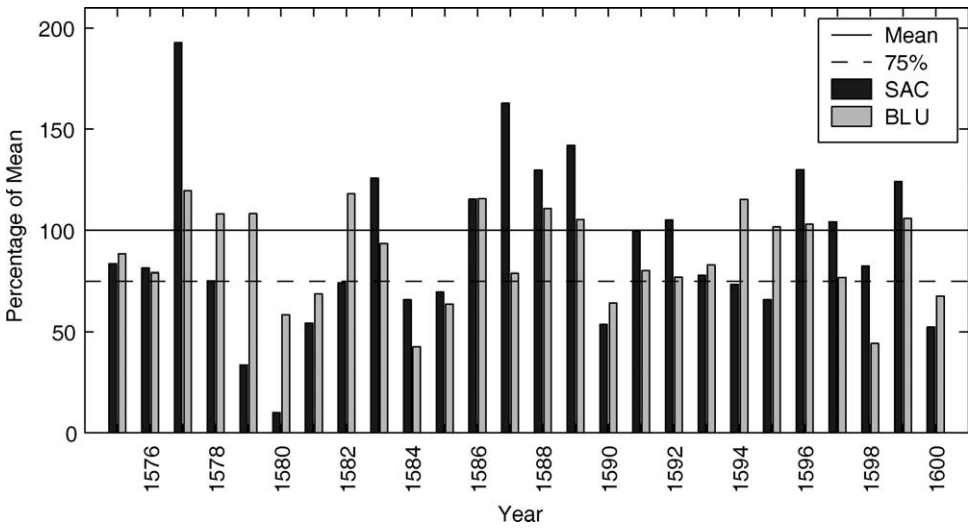

Fig. 6. Bar plot showing annual reconstructed flow anomalies on SAC and BLU in late 1500s. Values plotted as percentage of 1916–1977 mean of reconstructed flow. Horizontal dashed line is arbitrary drought threshold at 75% of mean.

characterized as decades-long unbroken drought on either SAC or BLU, but as a series of drought impulses broken by wet years (Fig. 6). The period 1586–1589 is in fact wetter than normal in both basins. Neither river is reconstructed below normal for more than five consecutive years. Longest stretches of below-normal are 5 yr (1578–1582) for SAC and 4 yr (1590–1593) for BLU.

Tree-ring anomalies for the six most severe joint-drought years in the period 1576–1600 are mapped (Fig. 7). These years—1580, 1581, 1584, 1585, 1590, and 1600—are the only years in this period in which reconstructed flow is less than 75% of the 1916–1977 mean on both rivers. To emphasize broad patterns, the anomalies are coded on the map by quartile: lower quartile, upper quartile, or middle two quartiles of tree-ring index. The base period 1575–1964 common to all chronologies was used for computing quartiles. The growth anomaly patterns for the 6 yr are quite dissimilar and point to no unique spatial footprint of moisture departure for extreme joint drought. Drought in the 6 yr, except for 1581, appears to be spatially contiguous across the Great Basin from BLU to SAC.

The year 1580, which is the record low reconstructed flow for SAC, is characterized by a SW/NE banding of dryness across the western United States, with evidence of moist conditions to the far northwest (Washington) and southeast (Arizona). Perhaps unusually persistent circulation patterns blocked storms through the central region while letting storms pass to

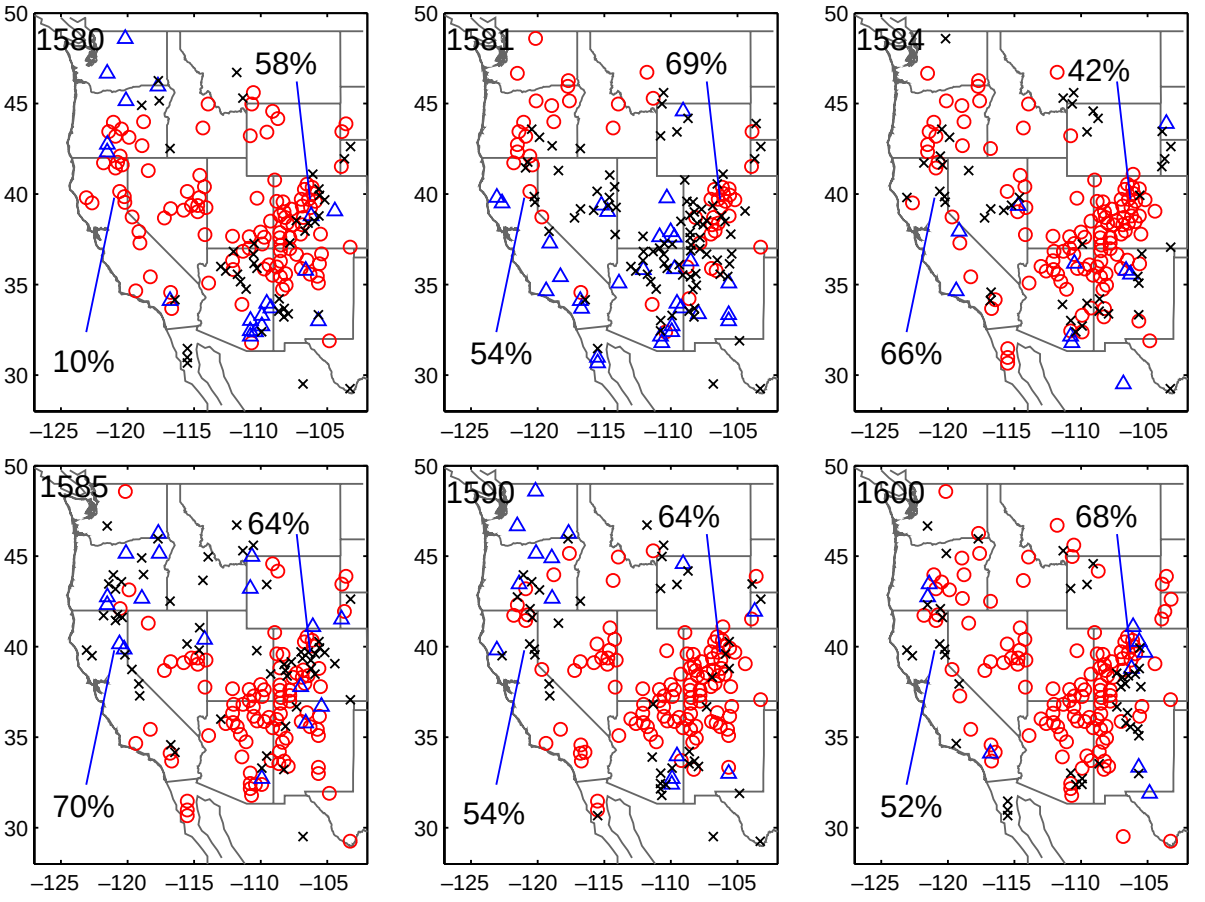

Fig. 7. Maps of annual tree-ring anomalies during joint-drought years of the late 1500s. Red circle for chronology in lowest quartile of growth; blue triangle in highest quartile; black '*x*' in middle two quartiles. Reconstructed flows for SAC and BLU each year are annotated as a percentage of 1916–1977 mean.

the north and south. A similar spatial pattern reappears in 1590, except that the dry zone is shifted slightly southward and, unlike in 1580, now encompasses Baja California. The dry band appears shifted even further south in 1585, when tree-ring indices are consistently low across the southern extreme of the study area.

In contrast, 1581 exhibits a north-centered drought, with growth departures well above normal across the southern third of the study area. It appears that both the Sacramento and Blue watersheds are just far enough north to be under the suppressed-rainfall regime in 1581. The years 1584 and 1600 present a separate type of spatial pattern in which tree-growth is generally suppressed over the entire western United States; the few tree-ring chronologies in the high-growth quartile in those years are scattered about in no organized pattern.

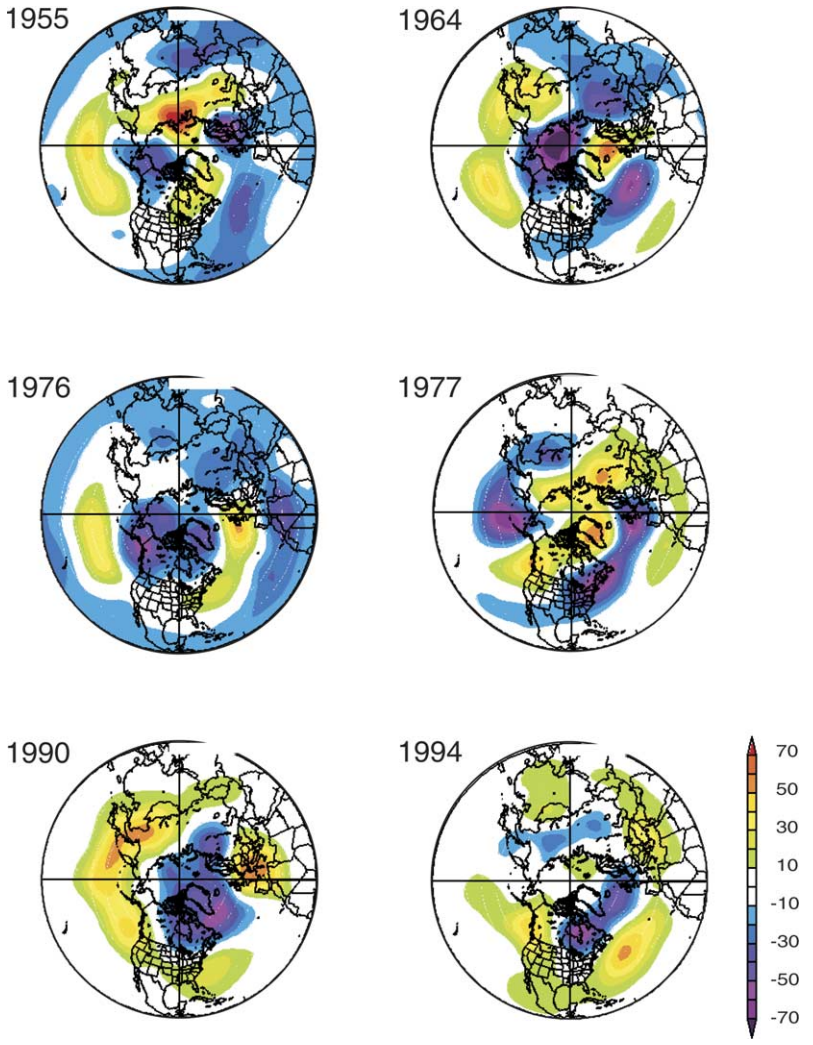

Fig. 8. Geopotential height anomalies (500 mb, October–May, based on 1948–1996) in 6 yr with joint droughts at less than the 0.25 quantile in observed SAC and BLU. Quantiles computed on 1916–2002.

5.4. Climatological factors

Widespread drought encompassing SAC, BLU, and intervening regions must be associated with unusual blocking patterns that persistently shunt precipitation-producing storms from large parts of the western United States. To infer the particular circulation anomalies that might be linked with joint droughts such as those of the late 1500s, we identified analog years in the 20th century from the observed flow records, 1916–2002, and summarized the circulation in terms of the anomalous 500-mb geopotential height field.

Streamflow was less than the 25th percentile in both SAC and BLU in 9 yr during 1916–2002. Six of these years (1955, 1964, 1976, 1977, 1990, 1994) are recent enough that the accompanying 500 mb patterns can be examined (Fig. 8). Maps shown are for the cool season (October through May), which is most important to runoff production in the watersheds. A common feature in all 6 yr is high pressure over the North Pacific Ocean and/or the Pacific Northwest. The first three years, 1955, 1964, and 1976, are characterized by a high centered over the north Pacific. In 1955 and 1964, a sequence of high and low pressure from the north Pacific, across northern Canada to the north Atlantic/Greenland suggests a cool season storm track north of most of the United States. In 1976, the high over the north Pacific is accompanied by a large area of low pressure over the North American Arctic. The patterns in both 1990 and 1994 include broad bands of high pressure. In 1990, high pressure extends from northern Asia across the north Pacific, and more weakly across the US, while in 1994, strong high pressure is centered in the Pacific Northwest, and weak high pressure covers all of North America except the Great Lakes and north into eastern Canada. In both of these years, low pressure over the eastern half of Canada in combination with the extensive high pressure resulted in wet conditions in the eastern US and dry conditions over much of the western United States. The 500 mb conditions in 1977, the most severe joint drought year, are the most unlike any of the other five joint-drought years. The pressure pattern exhibits a classic winter Pacific Northern American (PNA) configuration, low

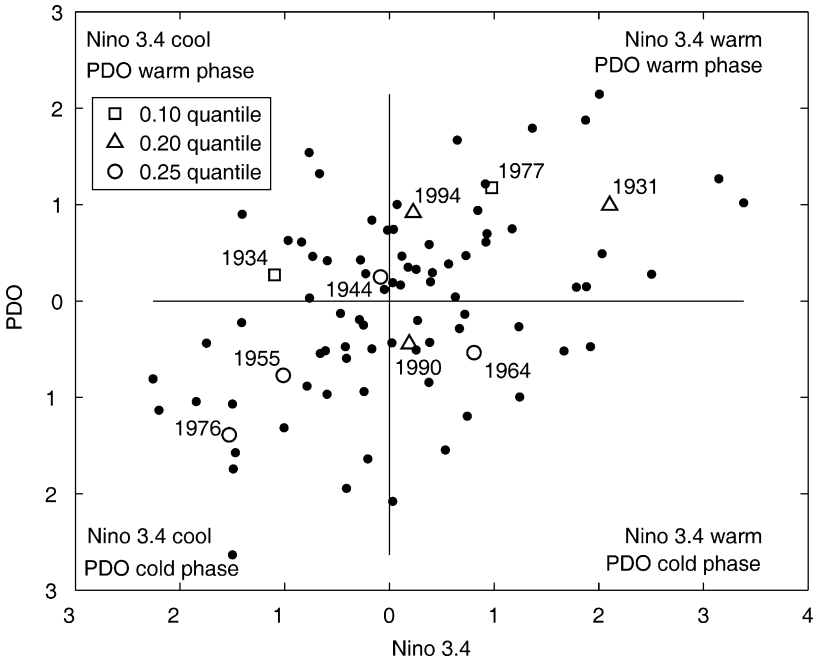

Fig. 9. Joint-drought years annotated on scatterplot of Pacific Decadal Oscillation (PDO) against eastern equatorial Pacific SST (Nino 3.4 index), 1916-2002. Joint drought defined is as water-year total flows of SAC and BLU simultaneously below specified quantile. Quantiles computed on 1916-2002 data.

pressure over the Aleutian Islands, high over the western Canada, and low over the eastern US (Wallace and Gutzler, 1981). In fact, the highest October–May PNA index value in the period 1950–2002 was recorded in 1977 (NOAA, 2003b). The strong high anchored over western British Columbia blocked the storm track from crossing the west coast of the US, leaving the western United States dry, but allowing moisture into regions east of the Continental Divide.

Anomalous sea-surface temperature (SST) patterns in the eastern Pacific Ocean have frequently been associated with climatic anomalies over western North America (Redmond and Koch, 1991; Cayan and Webb, 1992; Mantua et al., 1997; Gershunov and Barnett, 1998). A comparison of the observed flow records with Pacific SST indices suggests that joint droughts in SAC and BLU can occur under greatly contrasting SST scenarios. The orientation of the cloud of points in a scatterplot of the PDO index and the Niño 3.4 index (Trenberth and Stepaniak, 2001), for the years with observed flow data for SAC and BLU, 1916–2002 (Fig. 9) reflects the well-documented interdependence of PDO and ENSO phenomena (Gershunov and Barnett, 1998). Cool eastern equatorial Pacific generally occurs with cool-phase PDO, and vice versa. As shown by the annotated joint-drought years, no systematic relationship between joint drought and these SST indices is evident. The nine joint-drought years are distributed almost evenly among the quadrants of PDO and Niño 3.4 variability. Moreover, in none of the quadrants are the extreme occurrences of PDO/Niño 3.4 combinations joint-drought years.

The 2 yr identified as the most severe cases of joint drought—1934 and 1977—occurred in warm-phase of the PDO but with opposite-sign Niño 3.4 anomaly. The only back-to-back sequence of joint-drought years (1976 and 1977) was associated with greatly contrasting SST patterns: cool-phase in 1976 and warm-phase in 1977 by both SST indices.

The reconstructed flow series are broadly consistent with the observed flow series as far as the joint-drought years annotated in Fig. 9. The reconstructions cover the period through 1977, which encompasses seven of the nine annotated joint droughts, and all seven are years of below normal reconstructed flow on both rivers. The reconstructions prior to the start of the observed BLU flow record in 1916 imply that joint drought was rare early in the 20th century. In the period 1901–1916, only 1 yr (1913) was reconstructed with SAC and BLU both in their lowest tercile. Precipitation records also indicate that the early 1900s was exceptionally wet in the western United States (Bradley et al., 1982).

6. Summary and conclusion

The SAC and BLU streamflow reconstructions summarize long-term hydrologic variations in two major interdependent western United States watersheds. An analysis of the reconstructions provides a perspective on the relationships between flows in these two basins, especially with regard to joint droughts, over the last five centuries. Although flow for SAC and BLU are only very weakly correlated over the full 538-yr reconstruction period, more years of joint drought occur than would be expected by chance alone, including droughts of extreme severity in both watersheds. In the gage record, on the other hand, the frequency of joint-drought years is significant only for moderate drought years (0.5 quantile). This suggests that while climate controls on streamflow are generally different in the two watersheds, there may be a tendency for controls in some drought years to be more widespread, and is consistent with results of Cayan et al. (2003). The large spatial extent of moisture deficits in joint-drought years is supported to some degree by the maps of patterns of growth departure of moisture-sensitive tree-ring widths for joint-drought years in the late 16th century.

Although weak over the full reconstruction period, the relationship between streamflow in the two basins appears to be variable over time. There are periods, such as the late 16th century, and much of the 18th century, when reconstructed flow in the two basins is significantly correlated. These periods correspond to episodes of joint drought as revealed by smoothed (late 16th century) and/or unsmoothed (18th century) analysis of time series. Some joint droughts, however, occur outside the periods of high inter-basin correlation in flows. The intervals of time when flow is more closely correlated between the two basins are characterized by coherency at frequencies that include what is commonly defined as the ENSO band. This

band is so broad, however, that it is difficult to point to an unambiguous link. Coherence in the ENSO band is only faintly indicated in the 20th century, suggesting mechanisms driving synchrony may have been different in the past. Joint droughts in instrumental gage records, when compared to Pacific SST indices, do not indicate any consistent relationship between joint drought and ENSO or PDO in the 20th century, but perhaps forcing mechanisms related to or similar to ENSO were more influential during some periods in the past.

The reconstructions provide both an extended record that may allow a more robust assessment of statistical significance, as in the case of frequency of joint-drought events, and enable an evaluation of the representativeness of the gaged record in a longer context. For example, as mentioned above, we find that the covariation in reconstructed flows was stronger in the late 1500s and mid-1700s than at any time since 1800.

Water supply management and planning will be increasingly challenged by growing demand due to economic and population growth, and compounded by natural climate variability and anthropogenically induced climate change. Effective planning will require an understanding of long-term natural variability. Information about regional patterns of climate variability over decadal time scales provides information on possible controls on water supply in basins across a region. The extended tree-ring based reconstructions allow an assessment of the long-term character of steamflow and climate variability, and play a key role in broadening our understanding of western United States water supply variability and the controls on it. This work presents an example of how an analysis of available paleoclimatic reconstructions and data can begin to expand knowledge about widespread drought, frequency, distribution over time, and implications of causal mechanisms.

Acknowledgements

This research was supported by grants ATM-0080834 and ATM-0080889 from the National Science Foundation and from NOAA Office of Oceanic and Atmospheric Research, Climate Change Data and Detection program grant RA1330-02-AE-0037. We thank contributors to the ITRDB for making their data available.

References

Bloomfield, P., 2000. Fourier Analysis of Time Series: An Introduction, second ed. Wiley, New York.

Bradley, R.S., Barry, R.G., Kiladis, G., 1982. Climatic Fluctuations of the Western United States During the Period of Instrumental Records, Contribution No. 42, Department of Geology and Geography, University of Massachusetts, Amherst, Mass. 01003-00026 1982.

CADWR, 2003. California Department of Water Resources, WSIHIST, available: http://cdec.water.ca.gov/cgi-progs/iodir/wsihist (Accessed 30/6/03).

Cayan, D.R., Peterson, D.H., 1989. The Influence of North Pacific Atmospheric Circulation on Streamflow in the West: Geophysical Monograph 55. American Geophysical Union pp. 375–397.

Cayan, D.R., Webb, R.H., 1992. Coupled climate model simulation of el Niño/southern oscillation: implications for paleoclimate, in: Diaz, H.F., Markgraf, V. (Eds.), el Niño: Historical and Paleoclimatic Aspects of the Southern Oscillation. Cambridge University Press, Cambridge, pp. 29–68.

Cayan, D.R., Dettinger, M.D., Redmond, K.T., McCabe, G.J., Knowles, N., Peterson, D.H., 2003. The transboundary setting of California's water and hydropower systems: linkages between the Sierra Nevada, Columbia and Colorado hydroclimates, in: Diaz, H.F., Morehouse, B.J. (Eds.), Climate and Water: Transboundary Challenges in the Americas. Kluwer, Dordrecht, pp. 237–262.

Chatfield, C., 1975. The Analysis of Time Series, Theory and Practice. Chapman & Hall, London pp. 263.

Conover, W., 1980. Practical Nonparametric Statistics, second ed. Wiley, New York.

Cook, E.R., Briffa, K., Shiyatov, S., Mazepa, V., 1990. Tree-ring standardization and growth-trend estimation, in: Cook, E.R., Kairiukstis, L.A. (Eds.), Methods of Dendrochronology, Applications in the Environmental Sciences. Kluwer, Dordrecht, pp. 104–123.

Crippen, J.R., 1986. California; surface-water resources, in: Moody, D.W., Chase, E.B., Aronson, D.A. (Eds.), National Water Summary 1985—Hydrologic Events and Surface-water Resources, United States Geological Survey Water-Supply Paper 2300. United States Government Printing Office, Washington, DC, pp. 157–166.

Dawdy, D.R., Matalas, N.C., 1964. Statistical and probability analysis of hydrologic data, part III: analysis of variance, covariance and time series, in: Chow, V.T. (Ed.), Handbook of Applied Hydrology, A Compendium of Water-Resources Technology. McGraw-Hill Book Company, New York, pp. 8.68–8.90.

Dracup, J.A., Kahya, E., 1994. The relationships between U.S. streamflow and la Niña events. Water Resources Research 30 (7), 2133–2141.

Enfield, D.B., 1992. Historical and prehistorical overview of el Niño/Southern Oscillation, in: Diaz, H.F., Markgraf, V. (Eds.), el Niño: Historical and Paleoclimatic Aspects of the Southern Oscillation. Cambridge University Press, Cambridge, pp. 95–117.

Gershunov, A., Barnett, T.P., 1998. Interdecadal modulation of ENSO teleconnections. Bulletin of the American Meteorological Society 79 (12), 2715–2725.

Gershunov, A., Schneider, N., Barnett, T., 2001. Low-frequency modulation of the ENSO—Indian Monsoon rainfall relationship: signal or noise?. Journal of Climate 14, 2486–2492.

Gleick, P.H., Nash, L., 1991. The Societal and Environmental Costs of the Continuing California Drought. Pacific Institute for Studies in Development, Environment, and Security, 1681 Shattuck Avenue, Suite H, Berkeley, CA 94709 pp. 66.

Hulme, M., 2000. Datasets/Global precipitation, available: http://www.cru.uea.ac.uk/~mikeh/datasets/global/ (Accessed 03/6/2003).

Hulme, M., Osborn, T.J., Johns, T.C., 1998. Precipitation sensitivity to global warming: comparison of observations with HadCM2 simulations. Geophysical Research Letters 25, 3379–3382.

IPCC, 2001. Climate Change 2001: Synthesis Report. A contribution of Working Groups I, II and III to the Third Assessment Report of the Intergovernmental Panel on Climate Change, Watson, R.T., and The Core Writing Team (Eds.), Cambridge University Press, Cambridge, UK, pp. 398.

Julian, P.R., Chervin, R.M., 1978. A study of the southern oscillation and Walker circulation phenomenon. Monthly Weather Review 106, 1433–1451.

Loomis, J., Koteen, J., Hurd, B., 2003. Economic and institutional strategies for adapting to water resource effects of climate change, in: Lewis Jr.., W.M. (Ed.), Water and Climate in the Western United States. University of Colorado Press, Boulder, pp. 235–249.

Mantua, N.J., 2003. PDO Paper, available: http://www.atmos.washington.edu/~mantua/abst.PDO.html (Accessed 30/6/2003).

Mantua, N.J., Hare, S.R., Zhang, Y., Wallace, J.M., Francis, R.C., 1997. A Pacific interdecadal climate oscillation with impacts on salmon production. Bulletin of the American Meteorological Society 78, 1069–1079.

Meko, D.M., 2001. Reconstructed Sacramento River system runoff from tree rings, Report prepared for the California Department of Water Resources under agreement No. B81923-SAP # 4600000193: Tucson, Arizona, available from: California Department of Water Resources, P.O. Box 942836, Room 1601, Sacramento, CA 94236-0001.

Meko, D.M., Therrell, M.D., Baisan, C.H., Hughes, M.K., 2001. Sacramento River flow reconstructed to A.D. 869 from tree rings. Journal of the American Water Resources Association 37 (4), 1029–1040.

NOAA, 2003. World Data Center for Paleoclimatology, National Climatic Data Center. Climate Reconstructions, Sacramento and Blue River (under TreeFlow Project) reconstructions, available:http://www.ngdc.noaa.gov/paleo/recons.html (Accessed 30/06/2003).

NOAA, 2003. Climate Prediction Center, National Weather Service. Monthly and Atmospheric SST Indices, http://www.cpc.noaa.gov/data/indices/ (Accessed 8/8/2003).

NOAA, 2003. Climate Diagnostics Center, Office of Ocean and Atmospheric Research. Interactive Plotting and Analysis Pages, available:http://www.cdc.noaa.gov/cgi-bin/PublicData/getpage.pl (Accessed 10/8/2003).

NOAA 2003. World Data Center for Paleoclimatology, National Climatic Data Center. International Tree-Ring Data Bank, Tree-Ring Data, available: http://www.ngdc.noaa.gov/paleo/treering.html (Accessed 10/8/2003).

Redmond, K.T., Koch, R.W., 1991. Surface climate and streamflow variability in the western United States and their relationship to large-scale circulation indices. Water Resources Research 27, 2381–2399.

Rider, E., 2003. Three is not a charm: Waternews, 22, 3–4. Northern Colorado Water Conservancy District, Loveland, CO.

Snedecor, G.W., Cochran, W.G., 1989. Statistical Methods, eighth rev. ed., Revised by Iowa State University Statistics Department Staff Iowa State University Press.

Stahle, D.W., et al., 2000. Tree-ring data document 16th century megadrought over North America. EOS Transactions 81 (12), 121–125.

Stepaniak, D.P., 2002. TNI and N3.4, available: http://www.cgd.ucar.edu/cas/catalog/climind/TNI_N34/index.html (Accessed 30/6/2003).

Trenberth, K.E., Stepaniak, D.P., 2001. Indices of el Niño evolution. Journal of Climate 14, 1697–1701.

Wallace, J.M., Gutzler, D.S., 1981. Teleconnections in the geopotential height field during the Northern Hemisphere winter. Monthly Weather Review 109, 784–812.

Woodhouse, C.A., Webb, R.S., Lukas, J.J., 2003. Using dendrohydrologic data in Colorado water resource planning and management: Abstracts Volume, 83rd American Meteorological Society Annual Meeting, Long Beach, CA, February 10–13 2003 pp. 67.